Raman Characterization of the Phase Transition of Ion Implanted Hexagonal Boron Nitride to cubic Boron Nitride Nanoparticles

E. Aradi, S. R. Naidoo, R. M. Erasmus, T. E. Derry

School of physics, University of the Witwatersrand and DST/NRF Centre of Excellence

Private Bag 3, Wits 2050, Johannesburg, South Africa

395719@students.wits.ac.za

Abstract

We investigated the phase transition of hexagonal boron nitride (h-BN) to the c-BN form by the ion implantation process. Raman Spectroscopy was the major technique used in the characterization of the possible h-BN - c-BN phase transformation. The hexagonal BN samples were implanted with various ions including helium, lithium and boron, at different ion fluences ranging from 1×10^{16} ions/cm^2 to 1×10^{16} ions/cm^2. The effect of varying the ion implantation energies ranging from 40 keV to 160keV were also investigated on samples implanted by helium ions. Finally lithium implanted samples was studied using the 488 nm and 514 nm Raman laser lines. Micro Raman spectroscopy (μ-RS) measurements indicated that indeed ion implantation induced a phase change to the h-BN, evident from the longitudinal optical (LO) peaks at wavenumbers 1298 cm^{-1} and 1304 cm^{-1} appearing in the spectra after implantation. The nature and extent of these new peaks, and their dependence on the different implantation parameters is discussed.

1 Introduction

Due to its structure and bonding, c-BN exhibits excellent properties which make it very important in various applications [1, 2, 3, 4, 5].It exhibits hardness values of 70 GPa, second only to diamond's 100 Gpa [6, 7], as such it is an important material for abrasive processes and as a sintered ceramic for sawing, cutting, drilling or crushing applications. It has high thermodynamic stability at high pressures, with high melting point (3000 K) and thermal conductivity (13 Wcm^{-1}K^{-1}), second to diamond (4273 K) and 20 Wcm^{-1}K^{-1}) respectively. It also has low dielectric constants making it useful in high temperature high frequency microelectronic device fabrication [7, 8]. It is the lightest known group III-V compound with the widest band gap of E$_g$= 6.0-6.5 eV of all semiconductors [9, 10]. Its high refractive index (n$_{c-BN}$)=2.17) and a high transparency in a wide region of the electromagnetic spectrum enables it to be used in the fabrication of opto-electronics and electron emitting devices [11, 12].

It also surpasses diamond is with respect to oxygen stability and chemical inertness at elevated temperatures. Cubic BN's oxidation (1400 K) and phase change temperatures to h-BN (1700 K) are much higher than the oxidation temperature (900 K) and phase change temperature to graphite (1100 K) of diamond [13]. Cubic BN also shows high chemical inertness with molten ferrous materials at high temperatures of up to 1700-1800 K, whereas diamond readily forms iron carbide (Fe$_3$C$_2$) at these temperatures. This property makes c-BN very important in coatings and tribological applications of ferrous materials [14, 15, 16]. It can also be doped as both the p-type and n-type semiconductor making it superior to diamond whose shallow n-type semiconductor is still problematic [8]. This makes it useful in high speed electronic applications [17, 18], for example in the creation of p-n junction diode having a portion of its emission spectrum in the UV region [19, 20].

The excellent properties exhibited by c-BN leading to its enormous potential application have motivated researchers towards finding ways of synthesizing it. This research has been ongoing for the past half a century after its discovery in the late 1950's. To date, c-BN has been commercially synthesized in large quantities as powder by high pressure, high temperature method (HPHT) by Wentorf Jr [21].

The major setback in the c-BN synthesis has been the ability to produce large c-BN grains. As such it has been produced as thin films by Ion Beam Assisted Depositions IBAD techniques such as Chemical Vapour Deposition (CVD) and Physical Vapour Deposition (PVD).Current research is being focused development of thin c-BN films by role of defects, with h-BN as a starting material. Extensive research has been done theoretically [22] and experimentally [23, 24, 25] and concluded that defects induced in h-BN led to a phase transition to the c-BN phase. The work presented herein focused on optimizing the ion implantation conditions such as ion mass, implantation energies, ion fluence and temperature for c-BN growth during the ion implantation process.

2 Experiment

2.1 Sample and sample preparation

Hot pressed *h*-BN samples were used as the starting material throughout this work. The samples were supplied by Goodfellow UK Company limited as a 50 mm long and 15 mm in diameter rod. The rod was cut into 2 mm thick slices using a diamond wire saw with a wire thickness of 0.2 mm. The cut samples were then polished by a 1200 Å sand paper, ready for implantation.

2.2 Ion Implantation

All implantations were carried out at the iThemba Labs Gauteng, using the 200-20A2F ion implanter. The implanter consists of the ion source, where ions are produce, the analyzer magnet where ions with the specific m/q ratio are allowed to pass through for implantation, the accelerator which is able to accelerate ions at energies raging from 30 keV to 200 keV and the end station where the sample is located and where the implantation takes place. The implantation experiments were done at room temperature.

The first set of samples were implanted by varying the ion mass using He^+, Li^+ and B^+ at a the energy of 150 keV, and fluences ranging from 1×10^{14} ions/cm^2 to 1×10^{16} ions/cm^2. The second set were implanted with helium ions at the fluence of 5×10^{15} ions/cm^2, varying the implantation energy from 40 keV to 160 keV.

2.3 Raman Spectroscopy (RS)

All Raman measurements were performed in the in the Raman and Luminescence laboratory at the University of the Witwatersrand. The system consists of an argon ion-laser used in the excitation of the source, the Jobin- Yvon T64000 Raman triple grating spectrograph, and an optical microscope with a movable stage. A camera is attached to the microscope and the micrometer movement of the stage enables the study of the specimen on various positions.

Characterization of the samples was done before and after implantation in order to determine any structural changes. Measurements on the first two sets of samples were carried out at room temperature. Samples implanted with lithium ion were analyzed using the Ar^+ and Kr^+ laser lines. Cubic boron nitride powder samples were also analyzed by RS.
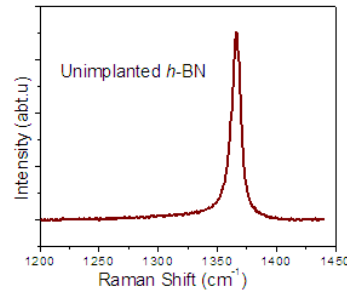
3 Results

3.1 unimplanted samples

.

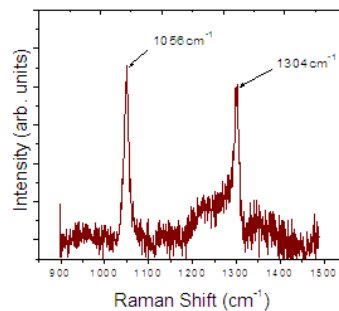Figure 1: Raman structure for unimplanted *h*-BN sample

Figure 2: Raman spectrum for *c*-BN sample

Due to the difference in the bonding nature of *h*-BN and *c*-BN, it is well expected that they will exhibit different Raman vibrational phonon mode signal. Figure 1 represents the spectrum for *h*-BN

sample before implantation. The spectrum clearly indicates a longitudinal optics (LO) $2E_{2g}$ phonon mode peak for h-BN at wavenumber $1366 cm^{-1}$, also reported by [26]. Figure 2 is a typical Raman signal for c-BN pressed crystal sample. Two phonon peaks observed at $1056 cm^{-1}$ and $1306 cm^{-1}$ represent the characteristic transverse optical (TO) and longitudinal optical (LO) modes respectively for the c-BN crystal, also reported by [3]. Our observations will be focused on the behaviour of the spectrum in figure 1 in comparison to features shown in figure 2.

3.2   Ion Mass Dependence

The ion mass dependence was achieved by implanting the h-BN sample using ions with different atomic masses, i.e. helium lithium and boron. Figures 3 shows the spectrum after implantation with the three ions.
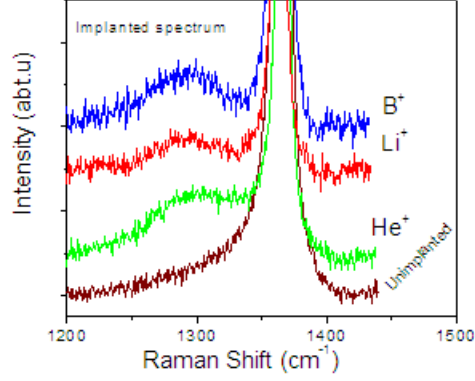

Figure 3: Spectrum of the implanted sample at higher resolution

Figure 3 is the spectrum at a higher resolution. From the figure **??**, it is evident that there is a new broad peak appearing after implantation. Its wavenumber vary from 1296 cm^{-1} for helium to 1299 cm^{-1} and 1303 cm^{-1} for lithium and boron respectively. This peaks are synonymous to the LO spectrum in figure 3 that occur at 1304 cm^{-1}, (although they are broader), predicting a possible ion induce phase transition to c-BN nanocrystals. The intensity of these peaks is dependent on the ion mass. This is evident from the spectrum of samples implanted by B^+ which gave a higher intensity signal with narrower peaks. The center was more towards the LO c-BN peak at lower fluence of 5×10^{14} ions/cm2. The other two ions had highest intensities at higher fluence i.e lithium at 1×10^{15} ions/cm2 and helium at 5×10^{15} ions/cm2. The peaks also asymmetrically broadened and shifted to lower frequencies as we moved away from the optimum fluence for all the three ions. This phenomenon of has been explained in line with Spatial Correlation Model developed by Parayanthal and Pallak [27], where it is proposed that a decrease in the crystal size causes a shift in the wavenumber to lower frequencies as well as a broadening and increase in the asymmetry of a given Raman peak. Due to the possible reduce crystalline quality of smaller crystals, no signal was observed at the for the TO mode of c-BN.
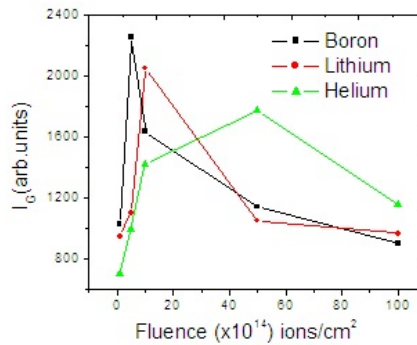

Figure 4: The Relationship between the Gaussian peak intensity and the ion fluence for boron lithium and helium.

From of the broad peaks obtained by varying the ion fluence, the peak intensities were normalized using a Gaussian peak fit. Figure 4 was then plotted as Gaussian peak intensity (I_G) as a function of the ion fluence. This was used for comparison for the three ions. There was a clear optimum fluence for each ion giving the highest peak intensities. Boron's peak intensity was highest towards lower fluence of the three ions while helium had the highest intensity at higher fluence.

3.3   Implantation Energy Dependence

Energy was varied for samples implanted with helium ions at the optimum dose of 5×10^{15} ions/cm^2 . Figure 5 shows the different spectra as obtained using energies from 40 keV to 160 keV
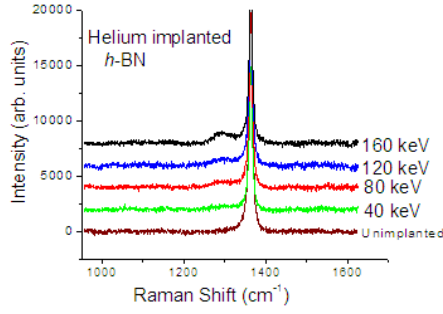
Figure 5: Raman spectrum of samples implanted by helium at with various energies

From figure 5, it is observed that at 40 keV, the c-BN Raman signal is almost completely faded, and hence the spectrum looks more or less as that of the unimplanted sample. As the energy increases to 80 keV, a weak signal is observed which slightly increases in intensity at 120 keV and finally it is more prominent at 160 keV. This energy dependence indicated that most of the energy lost by the ions as they penetrate matter is mainly due to electronic stopping which occurs at high energy regimes. This is well expected for helium ions since they are much lighter ions.
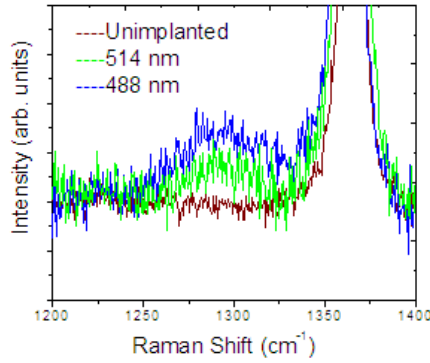
3.4   Raman Laser Dependence

Figure 6: Raman spectrum of samples implanted by lithium analyzed by different laser powers

The samples that were implanted with lithium ions at the optimum fluence of 1×10^{15} ions/cm2 were analyzed by two different Raman lines i.e. the 514 nm Ar^+ and the 488 nm Kr^+ line to determine which of the two laser lines was the most effective in c-BN analysis, and results shown in figure 6

Clearly the broad peaks are visible in the two spectra. The blue Kr^+ 488 nm line gave a stronger LO peak signal intensity as compared to the green 514 Ar^+ nm line. This shows that there is a dependence of the Raman signal to the laser power used.

4   Conclusions

From the results presented herein, it is proposed that ion implantation induced a phase change of h-BN to c-BN nanocrystals. This is is evident from the LO phonon peaks observed in samples after implantation. The effect of size reduction explains the broadening and the frequency shift from the known c-BN LO mode that occurs at 1306 cm^{-1}. This effect is caused by a possible high density stress caused by defects induced during implantation. Boron ion implantation gave the best Raman signals with its peaks being narrower and symmetrical as compared to lithium and helium. Boron also had the highest peak intensity at much lower fluence followed by lithium and finally helium. The experiments show that there is a high dependence of the possible c-BN nanocrystals production with the implantation energy. Lighter ions required high energy for the transformation as compared to heavier ones. Finally our experiments show that the laser line in the blue spectral region are most effective in the investigation of c-BN thin films. Future work will involve the use of other characterization techniques such as Transmission Electron Microscopy (TEM), Surface Brillouin Scattering (SBS) and X-ray Diffraction to complement Raman spectroscopy ascertaining this possible phase change.

5   Acknowledgements

References

[1] B. Mårlid, and K. Larsson, and J. O. Carlsson 1999 *Phys. Rev. B* **60**, 16055.

[2] Otfired Madelung 2004 *Springer- Verlag, Berlin Hedenburg* **3**, 755.

[3] W. J. Zhang, Y. M. Chong, I. Bello, S. T. LeeW. J. Zhang, Y. M. Chong, I. Bello, S. T. Lee 2007 *J. Phys. D Appl. Phy.* **40**, 6159.

[4] P. B. Mirkarimi, and K. F. McCarthy, and D. L. Medlin 1997 *J. Mater. Sci. Eng* **21**, 47.

[5] R. M. Erasmus and J. D. Comins and M. L. Fish 2000 Diam. Relat. Mater. **9**, 600.

[6] N. Ooi and A. Rairkar and L. Lindsey and J. B. Adams 2006 *Phys.: Cond. Matter Phys.* **18**, 97.

[7] J. Karlsson and K. Larsson 2010 *J. Phys. Chem.* **2**, 3516.

[8] S. Reich, S. and A. C. Ferrari and R. Arenal and A. Loiseau and I. Bello and J.Robertson 2005 *Phys. Rev. B.* **71**, 205201.

[9] J. Guo and H.Wang and K. Zheng and H. Yan and M. Yoshimura 2007 *Electrochemistry communication* **9**, 1824.

[10] C. B. Samantaray, and R. N. Singh 2005 *Int. Mater. Rev.* **50**, 313.

[11] W. Sekkal and B. Bouhafs and H. Aourag and M. Certier 1998 *J. Phys. Condens. Matter* **10**, 4975.

[12] C. Oshima and A. Nagashima 1997 *J. Phys. Condens. Matter* **9**, 9.

[13] H. Uchida and M. Yamashita and S. Hanaki and A. Kurihara 2008 *Mater. Sci. Engi.: A* **483**, 695.

[14] J. Zhang, and Q. Cui, and X. Li, and Z. He, and W. Li, and Y. Ma, and Q. Guan, and W. Gao, and G. Zou 2004 Phys. Rev. B, **399** 451.

[15] Z. Y. Nain, and Z. G. Tian, and Z.P. Wen 1999 *Chin. Rev. Lett* **16**, 155.

[16] C. Ronning and H. Feldermann and H. Hofsass 2000 *Diam. Relat. Mater.* **9**, 1769.

[17] Y. Yan, S. B. Zhang and M. M. Al-Jassim 2002 *Phys. Rev. B.* **66**, 201401.

[18] Albe Karsten 1997 *Phys. Rev. B.* **55**, 6203.

[19] C. X. Wang and Y. H. Yang and G. W. Yang 2004 *J. Phys. Chem. B .* **108**, 728.

[20] V. L. Solozhenko, and O. O. Kurakevych, and D. Andrault, and Y. Le Godec, and M. Mezouar 2009 *Phys. Rev. Lett.* **102**, 015506.

[21] R. H. J Wentorf 1957 *J. Chem Phys.* **26**, 957.

[22] T. E. Mosuang, and T. Lowther 2002 *Phys. Rev. B.* **63**, 014112.

[23] C. Hu and Q. M. J. Wu and J. Shen and S. Kotake and Y. Suzuki 2002 *Thin Solid Films* **402**, 117.

[24] R. Machaka, and R. M. Erasmus, and T. E. Derry 2010 *Diam. Relat. Mater* **19**, 11331.

[25] E. Aradi, R. M. Erasmus, T. E. Derry 2011 *In Press.*

[26] R. J. Nemanich, S. A. Solin, R. M. Martin 1981 *Phys. Rev. B.* **12** 6348.

[27] P. Parayanthal, F. H. Pollak 1984 *Phys. Rev. Lett.* **52(9)** 1822.